2011 IEEE International Conference on Robotics and Automation
Shanghai International Conference Center
May 9-13, 2011, Shanghai, China

On Two-Finger Grasping of Deformable Planar Objects

Yan-Bin Jia Feng Guo
Department of Computer Science
Iowa State University
Ames, IA 50011, USA
jia,fguo@cs.iastate.edu

Jiang Tian
Technicolor Visual Technology Co., Ltd.
Building B, 40 North-Middle 3rd Ring Road
Haidian District, Beijing 100088, P.R. China
jiangtian10@gmail.com

Abstract— **Grasping a deformable object instantaneously requires maintaining equilibrium of its pre- and post-deformed shapes using the same set of forces. This paper studies the type of grasps generated by squeezing a planar object with two fingers. It is shown that the success of such a grasp is independent of the applied forces in the case of small deformation. Numerical algorithms are introduced to compute sets of squeeze grasps with small and large deformations modeled using the finite element method (FEM) based on the linear and nonlinear elasticity theories, respectively.**

I. Introduction

Deformable objects are manipulated daily in our life. The ability to handle such objects constitutes an important measure of a robot's dexterity.

Among all manipulation operations, grasping is representative for its simplicity and robustness. A grasp of a rigid object achieves force closure if it can resist an arbitrary external wrench (force plus torque) exerted on the object. If any motion of an object is prevented, form closure is achieved. Nguyen's result [9] on two-finger grasping under point contact in the plane states that a grasp is force closure if the two contact friction cones contain the line segment connecting the two contact points. Ponce et al. [10] derived several necessary and sufficient conditions for force closure on polyhedral objects.

For deformable objects, the notion of form closure is inadequate as the object deforms with infinite many degrees of freedom. Also, grasp analysis and synthesis are no longer purely geometric problems. The wrench space will change as a result of varying shape geometry, which is determined by either solving a high order differential equation or minimizing the potential energy.

One difficulty in synthesizing a grasp of a deformable object is that *the very set of grasping forces must maintain equilibrium before and after the deformation, over the object's original and deformed shapes, respectively.* The pre- and post-deformation configurations cannot be analyzed separately using geometric techniques developed for rigid body grasping which would presume independent sets of forces for the two configurations. Equilibrium of the post-deformed shape has to be maintained by the same forces that generated it, otherwise it would be a violation of the physics of deformation (described by the elasticity theory).

The other difficulty lies in the need for obtaining deformed shapes under various finger placements in the search for a grasp, despite the non-existence of closed-form descriptions. The high cost in deformation modeling presents an obstacle for efficiently constructing a grasp.

This paper studies how to grasp a planar object by squeezing it with two fingers moving toward each other. The fingers have curved tips that make point contacts with the object. The object is physically linear (governed by Hooke's law) but geometrically either linear or nonlinear. We assume that deformation happens instantaneously rather than in a duration so dynamic effects are ignored. Also, this relieves us from worrying about the same forces staying balanced throughout the deformation period.

The paper is organized as follows. Section II surveys related work on grasping of rigid and deformable objects. Section III defines the grasp of a deformable object and establishes necessary and sufficient conditions for two-finger grasps. Section IV describes algorithms that compute sets of finger placements to grasp an object. Section V goes over computation of the deformed shape using FEM based on linear and nonlinear elasticity theories. Simulation examples are then presented in Section VI. This is followed by some discussion in Section VII.

II. Related Work

Grasping of rigid objects has been extensively studied in the last two decades [1]. Such grasps are classified as either force or form closure[1], for which grasp analysis is geometric and grasp synthesis algorithmic.

Two-fingered force-closure grasps of a polygon are well characterized and efficiently computable [9]. For a piecewise-smooth curved 2D object, Ponce et al. [11] utilized cell decomposition to compute pairs of maximal-length graspable segments. Two fingers can be positioned independently in the interior of a pair of such segments to guarantee force closure. Blake [2] classified planar grasps into three types using a symmetry set, an anti-symmetry set, and a critical set. Jia [5] presented a fast algorithm that computes all pairs of antipodal points on a planar curved object.

An $O(n^2 \log n)$-time algorithm was proposed in [8] to compute an optimal three-finger planar grasp by maximizing the radius of a disk centered at the origin and contained in the convex hull of the three unit normal vectors at the finger contacts. Assuming rounded fingertips, an optimality measure

[1] Form closure can be viewed as force closure with frictionless contact.

of force-closure grasps was introduced in [7] where efficient algorithms were presented for polygons and polyhedra.

Sinha and Jacob [12] introduced a model for deformable contact regions under a grasp that predicts normal and tangential contact forces based on nonlinear energy optimization. Their work was not concerned with how to compute or achieve such a grasp, neither did it model the change in global geometry of the grasped object. Luo and Xiao [6] derived geometric properties of deformable contacts that are useful for improving physical accuracy and simulation efficiency. The recent work by the authors [13] studied deformable modeling of shell-like objects on which grasps were also assumed to have been achieved already. It assumed point contacts and modeled the grasped object's global shape change.

Design of grasp strategies for deformable objects has attracted the attention of robotics researchers in more than a decade. Wakamatsu et al. [14] proposed the concept of bounded force-closure for deformable objects. Hirai et al. [4] used both visual and tactile information to control the motion of a deformable object.

Manipulation planning of deformable objects was presented by Wakamatsu and Hirai [15] for linear objects. Gopalakrishnan and Goldberg [3] introduced the deformation-space (D-space) of an object, with modeling based on linear elasticity and frictionless contact.

Most of the above methods have assumed linear elastic models, which is geometrically inexact for large deformations.

III. Grasp Definition and Squeeze Grasp

To grasp a deformable object, a finger placement needs to prevent any Euclidean motion of the object such that the only possible displacement is deformation. In the presence of friction, a force-closure grasp constrains a rigid object completely. Thus a necessary condition for a grasp on a deformable object is that *the grasp would be force closure on a rigid object of the same shape.* Here, uniform mass density is assumed.

Like in classical elasticity theories, dynamics are ignored in modeling deformation. It is reasonable to make the following quasistatic assumption about the grasp.

(A1) Deformation happens instantaneously such that the applied contact forces do not vary during this physical process, and no velocity of the object builds up.

We also ignore the effect of the gravitational force.

The success of a grasp satisfying the necessary condition can then be determined based on the object's post-deformation geometry and the original forces now applied at the displaced locations of the same finger contacts. No slip may happen during the deformation in order for the grasp to succeed. Under instantaneous deformation, this is guaranteed if the grasping forces stay inside their respective contact friction cones before and after the deformation. The object, in its deformed shape, needs to be constrained from any rigid motion and maintained at equilibrium by the same finger placement. The applied forces by these fingers must not vary though, otherwise the object will continue to deform, making the equilibrium analysis invalid.

Definition A finger placement exerting a set $\mathcal{F}$ of forces on a deformable object $\mathcal{B}$ is a *grasp* if the same finger placement (i.e., with no movement along the object's boundary) would maintain equilibrium by exerting $\mathcal{F}$ on both

1) a rigid object of $\mathcal{B}$'s pre-deformation shape; and
2) another rigid object of $\mathcal{B}$'s post-deformation shape.

In this paper, we consider grasps by two fingers squeezing a planar object with curved boundary. The following assumptions are made about contact and fingertips.

(A2) The fingers make point contacts with the object in the presence of friction.

(A3) The fingertips are curved and convex (semi-circular, for instance).

The squeeze action is equivalent to keeping one finger still and stuck to its contact point, say, $\boldsymbol{q}$, while translating the other finger toward $\boldsymbol{q}$ without slip at its contact point, say $\boldsymbol{p}$.

(C1) The contact point $\boldsymbol{q}$ does not move in the plane.

The situation is illustrated in Fig. 1. We refer to the action as a *squeeze grasp*.

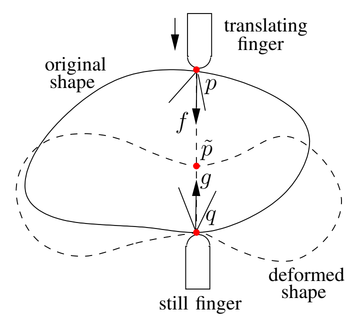

Fig. 1. Squeeze grasp.

Before deformation starts, the finger placement needs to be force closure to prevent any free motion of the object. This requires that the segment $\overline{\boldsymbol{pq}}$ be inside the friction cones at $\boldsymbol{p}$ and $\boldsymbol{q}$ [9]. As shown in Fig. 1, a force $\boldsymbol{f}$ is applied at $\boldsymbol{p}$.[2] To maintain initial equilibrium, $\boldsymbol{f}$ must be in the direction of $\boldsymbol{q}-\boldsymbol{p}$, and the reaction force $\boldsymbol{g}$ at $\boldsymbol{q}$ must satisfy $\boldsymbol{f}+\boldsymbol{g}=0$ so that the total wrench is zero. Otherwise, the forces would result in an Euclidean motion without deformation.

Denote by $\mathcal{G}(\boldsymbol{p},\boldsymbol{q})$ the finger placement at $\boldsymbol{p}$ and $\boldsymbol{q}$. The directions of the squeezing forces are thus determined and their magnitudes are equal. No slip may happen for a grasp to be achieved at the contact points $\boldsymbol{p}$ and $\boldsymbol{q}$. The tangents to the object at the two points are therefore collinear with those to the fingers, respectively. Hence the following geometric condition is satisfied by the deformation generated by a successful grasp.

(C2) The tangents at $\boldsymbol{p}$ and $\boldsymbol{q}$ do not rotate.

Conditions (C1) and (C2) will be used later as constraints for solution of the deformed shape.

[2]Note that the force includes a tangential component due to friction.

Due to instantaneous deformation, the forces $\boldsymbol{f}$ and $\boldsymbol{g}$ do not change their directions. To maintain equilibrium after the deformation, the displaced location $\tilde{\boldsymbol{p}}$ of $\boldsymbol{p}$ must lie on the line segment $\overline{\boldsymbol{pq}}$.[3]

Theorem 1: A finger placement $\mathcal{G}(\boldsymbol{p}, \boldsymbol{q})$ applying squeezing forces of magnitude f is a grasp if and only if the following two conditions are satisfied:

(G1) $\overline{\boldsymbol{pq}}$ lies inside the friction cones at $\boldsymbol{p}$ and $\boldsymbol{q}$ on the object's pre-deformation shape;

(G2) the displaced location $\tilde{\boldsymbol{p}}$ of $\boldsymbol{p}$ lies on the $\overline{\boldsymbol{pq}}$.

Proof: We first establish the sufficiency of the two conditions. Condition (G1) implies no slip at the start of deformation when the forces are applied. Since the contact point on the moving finger is translating toward $\boldsymbol{q}$, condition (G2) ensures that this point and $\boldsymbol{p}$ (on the object) move together, hence their contact sticks during the deformation. The still finger also sticks to its contact, since constraints (C1) and (C2) are applied in obtaining the deformed shape. Thus the contact friction cones will not rotate. The same pair of opposing forces will still be inside these cones after the deformation, which in turn guarantees no slip during the grasp.

The necessity can be easily shown by contradiction. Suppose that condition (G1) does not hold. Then no applied forces can achieve equilibrium even before deformation happens, let alone a grasp. Suppose condition (G2) does not hold. Then the upper finger contact will slip as the finger translates. The grasp at $\boldsymbol{p}$ and $\boldsymbol{q}$ will not be achieved. ■

Verifying condition (G2) involves computing the displaced location $\tilde{\boldsymbol{q}}$ (and possibly the deformed shape) using the elasticity theory.

IV. Grasp Synthesis

For small deformations, the linear elasticity theory applies. Whether a placement will result in a grasp is independent of the force magnitude.

Theorem 2: Under the linear elasticity theory, if a finger placement $\mathcal{G}(\boldsymbol{p}, \boldsymbol{q})$ squeezing a deformable object with forces of magnitude f achieves a grasp, then the same placement will result in a grasp with any force magnitude within the theory's application range.

Proof: Let $\tilde{\boldsymbol{p}}$ be the displaced location of $\boldsymbol{p}$ under squeezing forces of magnitude f. Thus $\tilde{\boldsymbol{p}}$ lies on the line segment $\overline{\boldsymbol{pq}}$. Condition (G1) holds.

We first show that $\boldsymbol{p}$ is displaced to a location $\hat{\boldsymbol{p}}$ on the segment $\overline{\boldsymbol{pq}}$ when the force magnitude changes to $f + \Delta f$ for small enough Δf. Under the linear elasticity theory, the new displacement is $\hat{\boldsymbol{p}} - \boldsymbol{p} = (1 + \Delta f/f)(\tilde{\boldsymbol{p}} - \boldsymbol{p})$. Since $\tilde{\boldsymbol{p}} - \boldsymbol{p}$ has the direction of $\boldsymbol{q} - \boldsymbol{p}$, so does $\hat{\boldsymbol{p}} - \boldsymbol{p}$. Hence $\hat{\boldsymbol{p}}$ lies on the ray from $\boldsymbol{p}$ to $\boldsymbol{q}$. Because of the small deformation required by the linear theory, it cannot move past $\boldsymbol{q}$, hence staying on $\overline{\boldsymbol{pq}}$. Condition (G2) still holds. The conclusion follows from Theorem 1. ■

Theorem 2 reduces grasp computation to a geometric problem for small applied forces.

[3]Throughout this paper, the tilde notation '~' always refer to the displaced location of a point.

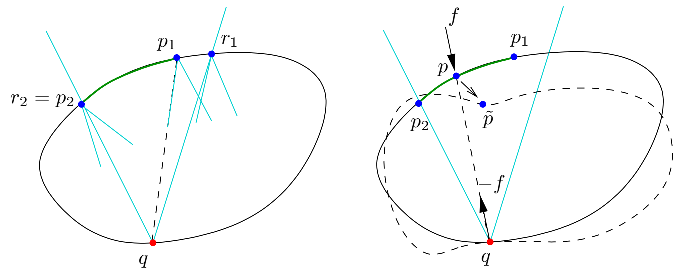

Fig. 2. Finding the segment of points forming a grasp with $\boldsymbol{q}$.

A. Fixed Contact for One Finger

Suppose one finger must stay in contact with a boundary point $\boldsymbol{q}$ of the deformable object. We would like to locate the other finger to form a grasp. Let the object's original boundary be described by the curve $\boldsymbol{\sigma}(s)$, where s is arc length. As shown in Fig. 2, we first find a boundary arc $\overset{\frown}{\boldsymbol{p}_1\boldsymbol{p}_2}$ on which every point $\boldsymbol{p}$ satisfies condition (G1) with $\boldsymbol{q}$. When $\boldsymbol{\sigma}$ is convex, this can be done in the following steps.

1. Intersect the edges of the friction cone at $\boldsymbol{q}$ with $\boldsymbol{\sigma}(s)$. Let the right and left intersections be $\boldsymbol{r}_1$ and $\boldsymbol{r}_2$, respectively.
2. If the friction cone at $\boldsymbol{r}_1$ contains $\boldsymbol{q}$, then let $\boldsymbol{p}_1 = \boldsymbol{r}_1$. Otherwise, march from $\boldsymbol{r}_1$ toward $\boldsymbol{r}_2$ on $\boldsymbol{\sigma}$ until it stops at a point $\boldsymbol{p}_1$ whose right friction cone edge passes through $\boldsymbol{q}$, or $\boldsymbol{r}_2$ is reached.
3. Find $\boldsymbol{p}_2$ via a symmetrical march from $\boldsymbol{r}_2$ toward $\boldsymbol{r}_1$.

The march in step (2) can be treated as finding a root of the equation $(\boldsymbol{q} - \boldsymbol{p}) \times \boldsymbol{e}_r(\boldsymbol{p}) = 0$ where $\boldsymbol{e}_r$ is the direction of the friction cone's right edge at $\boldsymbol{p}$. Note that the feasible segment $\overset{\frown}{\boldsymbol{p}_1\boldsymbol{p}_2}$ may not exist.

In case $\boldsymbol{\sigma}$ is not convex, we first split it at points of inflection into "monotone" segments on each of which the tangent rotates in one direction [5]. Then apply the algorithm described above on each monotone segment inside the friction cone at $\boldsymbol{q}$.

Every point $\boldsymbol{p} = \boldsymbol{\sigma}(s)$ on the arc $\overset{\frown}{\boldsymbol{p}_1\boldsymbol{p}_2}$ is displaced to some point $\tilde{\boldsymbol{p}} = \tilde{\boldsymbol{\sigma}}(s)$ under a squeezing force in the direction of $\boldsymbol{q} - \boldsymbol{p}$. Determining grasp existence becomes finding a root s of the equation

$$(\tilde{\boldsymbol{\sigma}}(s) - \boldsymbol{q}) \times (\boldsymbol{\sigma}(s) - \boldsymbol{q}) = 0. \tag{1}$$

This can be done numerically using either Newton's method, bisection, or by a march. At each iteration, the displaced location $\tilde{\boldsymbol{p}}$ is determined from recomputing the partial or entire deformed shape.

No grasp placing one finger at $\boldsymbol{q}$ exists if the algorithm finds no feasible arc $\overset{\frown}{\boldsymbol{p}_1\boldsymbol{p}_2}$ or no root of (1) on the arc.

B. Graspable Segments

Suppose a grasp $\mathcal{G}(\boldsymbol{p}_0, \boldsymbol{q}_0)$ exists. Consider relocating the lower finger to a point $\boldsymbol{q}$ slightly away from $\boldsymbol{q}_0$. With squeezing forces of the same magnitude, the root $\boldsymbol{p}$ of (1) must exist and be close enough to $\boldsymbol{p}_0$ under continuity of the physics for deformation. The friction cones at $\boldsymbol{q}$ and the displaced location $\tilde{\boldsymbol{p}}$ on the deformed shape will contain $\overline{\tilde{\boldsymbol{p}}\boldsymbol{q}}$.

Equation (1) thus locally defines the upper finger location $\boldsymbol{p}$ as a function of the lower finger location $\boldsymbol{q}$, in order to achieve a grasp. More formally, let $\boldsymbol{q}_0 = \boldsymbol{\sigma}(t_0)$, $\boldsymbol{p}_0 = \boldsymbol{\sigma}(s_0)$, and $\boldsymbol{q} = \boldsymbol{\sigma}(t)$. There exists a function $\omega(t)$ such that $\omega(t_0) = s_0$ and $\mathcal{G}(\boldsymbol{\sigma}(\omega(t)), \boldsymbol{\sigma}(t))$ is a grasp. The segment consisting of all such $\boldsymbol{q}$ surrounding $\boldsymbol{q}_0$ is called *graspable*.

Generally, the function ω is defined over disjoint intervals of the domain $[0, L)$ of the boundary curve $\boldsymbol{\sigma}(s)$. Each interval corresponds to a segment on which anywhere one finger is placed, the other finger can be property placed at some boundary location to form a grasp with it.

We can trace out the maximal graspable segment $\mathcal{P} = \boldsymbol{\sigma}[t_a, t_b]$ containing $\boldsymbol{q}_0$ as follows. Repeatedly, we place one finger at $\boldsymbol{\sigma}(t_1), \boldsymbol{\sigma}(t_2), \ldots$, where $t_i = t_0 + i\tau$ with a small step size τ on the object's boundary, and find locations $\boldsymbol{\sigma}(s_1), \boldsymbol{\sigma}(s_2), \ldots$ for the other finger, where s_{i+1} is searched in the neighborhood $[s_i - \varrho, s_i + \varrho]$ for some constant multiple ϱ of τ. Until s_{k+1} cannot be found, set $t_b \leftarrow t_k$. Similarly, we repeatedly test $t_0 - \tau, t_0 - 2\tau, \ldots$, to determine t_a.

To find all graspable segments, we discretize the object's boundary. Place one finger sequentially at each discretization point and use the procedure in Section IV-A to search for a location of the other finger for a grasp. For each grasp $G(\boldsymbol{p}_i, \boldsymbol{q}_i)$ found, use the procedure described above to trace out the graspable segments containing $\boldsymbol{q}_i$ and $\boldsymbol{p}_i$.

V. Computing the Deformed Shape

The grasping algorithms in Sections IV-A and IV-B require repetitively relocating one or two fingers on the boundary of an object and computing their locations after the resulting deformations. Generally, there exists no closed-form description of the deformed shape — it has to be computed numerically via minimizing the object's potential energy under the squeezing force.

A. Potential Energy Minimization

From now on, we focus on perhaps the simplest nontrivial class of isotropic objects. Every object from the class is swept out by a rectangular cross section along a 2-dimensional closed curve $\boldsymbol{\sigma}$ referred to as the *middle curve*. The cross section has width w and height h, both significantly less than the length of the curve. Fig. 3 shows a section of the object. Because of its small dimensions, the

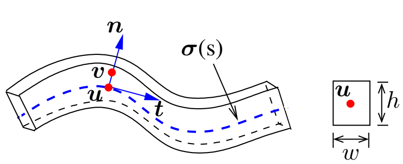

Fig. 3. Segment of a curve-like shape with rectangular cross section.

cross section assumes no deformation. So Poisson's ratio is zero. The shape is essentially a degenerated shell very small in two out of three dimensions. It can be used to approximate linear objects resting on a planar surface, for instance.

The middle curve $\boldsymbol{\sigma}(s)$ is parametrized by arc length, though computation easily carries over to an arbitrary-speed curve, as already shown for shells in our recent work [13]. We follow Kirchhoff's assumption that fibers initially normal to $\boldsymbol{\sigma}$ remain straight after deformation, do not change their lengths, and remain normal to the middle curve of the deformed geometry. The stress and strain at any point $\boldsymbol{v}$ inside the object can be represented in terms of those at the intersection point $\boldsymbol{u}$ of $\boldsymbol{\sigma}(s)$ with the normal section through $\boldsymbol{v}$. The displacement of $\boldsymbol{u}$ is best described in terms of its unit tangent $\boldsymbol{t}$ and unit normal $\boldsymbol{n}$ as $\boldsymbol{\delta}(s) = \alpha(s)\boldsymbol{t} + \beta(s)\boldsymbol{n}$.

For a small deformation, we obtain the extensional strain ϵ and the change in curvature ζ with a reduction of one dimension from those for shells [13]:

$$\begin{aligned} \epsilon &= \nabla_t \alpha + (\nabla_t \boldsymbol{n} \cdot \boldsymbol{t})\beta \;=\; \alpha' - \kappa\beta, && (2) \\ \zeta &= \nabla_t\left(-\nabla_t \beta + (\nabla_t \boldsymbol{n} \cdot \boldsymbol{t})\alpha\right) \\ &= -\beta'' - \kappa'\alpha - \kappa\alpha'. && (3) \end{aligned}$$

Here, $\nabla_t \alpha$ is the *directional derivative* of α with respect to $\boldsymbol{t}$, and $\nabla_t \boldsymbol{n}$ is the *covariant derivative* which measures the rate of change of the normal $\boldsymbol{n}$ along the middle curve at $\boldsymbol{p}$. The object's strain energy is represented as

$$U = \frac{1}{2} E w \int_0^L \left(h\epsilon^2 + \frac{h^3}{12}\zeta^2 \right) ds. \tag{4}$$

The linear component in the height h represents the extensional energy, while the cubic component represents the bending energy.

In the squeeze grasp shown in Fig. 1, one finger makes fixed contact at a boundary point $\boldsymbol{q}$, while the other applies a force $\boldsymbol{f}$ at another point $\boldsymbol{p}$ toward $\boldsymbol{q}$, displacing $\boldsymbol{p}$ to $\tilde{\boldsymbol{p}}$. The potential energy of the contact forces is

$$W = -\boldsymbol{f} \cdot (\tilde{\boldsymbol{p}} - \boldsymbol{p}). \tag{5}$$

The deformed middle curve $\boldsymbol{\sigma}(s) + \boldsymbol{\delta}(s)$, determined by the displacement field $\boldsymbol{\delta}$, minimizes the total potential energy

$$\Pi = U + W. \tag{6}$$

B. Finite Element Method

We discretize the middle curve $\boldsymbol{\sigma}$ into N finite (linear) elements. The problem of finding a minimizing displacement field $\boldsymbol{\delta}$ for the potential energy (6) reduces to that of determining the displacements $\boldsymbol{\delta}_i$ of the endpoints $\boldsymbol{p}_i$ (referred to as *nodes*) of these elements, $0 \le i \le N-1$.

The ith element $\overline{\boldsymbol{p}_i \boldsymbol{p}_{i+1}}$ has a parametrization $\boldsymbol{e}_i(u) = \sum_{j=i-1}^{i+2} b_j(u)\boldsymbol{p}_j$ over $[0,1]$ depending on four neighboring nodes. The coefficients $b_0, \ldots, b_{N-1}$ are chosen as cubic B-spline basis functions. The displacement of a point on the same element is $\boldsymbol{\delta}(u) = \sum_{j=i-1}^{i+2} b_j(u)\boldsymbol{\delta}_j$.

Following the standard FEM steps, over each element we use its displacement field to obtain strains (2) and (3), and substitute them into the strain energy (4). Extract out of the integral the products (all quadratic) of the coordinates of the nodal displacements $\boldsymbol{\delta}_{i-1}, \ldots, \boldsymbol{\delta}_{i+2}$, and integrate the remainder over the element domain $[0,1]$. Assembling over all elements, we can rewrite the strain energy into a matrix form: $U = \frac{1}{2}\boldsymbol{\Delta}^T K \boldsymbol{\Delta}$, where $\boldsymbol{\Delta} = (\boldsymbol{\delta}_0^T, \ldots, \boldsymbol{\delta}_{N-1}^T)^T$, and K is the $2N \times 2N$ *stiffness matrix*.

The nodes are numbered such that $\boldsymbol{p}_0$ and $\boldsymbol{p}_k$ are the lower and upper finger contacts $\boldsymbol{q}$ and $\boldsymbol{p}$, respectively, (see Fig. 1).[4] Meanwhile, let Q be the vector of forces exerted at the nodes $\boldsymbol{p}_0, \ldots, \boldsymbol{p}_{N-1}$, which are all zero but at $\boldsymbol{p}_0$ and $\boldsymbol{p}_k$. The potential energy of the applied forces is $W = -\boldsymbol{\Delta}^T Q$. The total potential energy (6) is minimized only if $\partial \Pi / \partial \boldsymbol{\Delta}$ vanishes, yielding the equation $K\boldsymbol{\Delta} = Q$ to be solved for the deformed shape.

C. Boundary Conditions and Efficient Grasp Computation

That $\boldsymbol{p}_0$ does not move provides two scalar constraints $\boldsymbol{\delta}_0 = 0$. No rotation of the tangent at $\boldsymbol{p}_0$ and $\boldsymbol{p}_k$, under finite-difference approximation of derivatives, become two equational constraints: $(\boldsymbol{\delta}_1 - \boldsymbol{\delta}_{N-1}) \cdot \boldsymbol{n}_0 = 0$ and $(\boldsymbol{\delta}_{k+1} - \boldsymbol{\delta}_{k-1}) \cdot \boldsymbol{n}_k = 0$, where $\boldsymbol{n}_0$ and $\boldsymbol{n}_k$ are the respective normals at the two points. These two constraints are exerted via two Lagrange multipliers λ_1 and λ_2. This yields an "enlarged" stiffness matrix K' of dimension $(2N+2) \times (2N+2)$ for $2N+2$ variables $\boldsymbol{\delta}_0, \ldots, \boldsymbol{\delta}_{N-1}, \lambda_1, \lambda_2$. Since $\boldsymbol{\delta}_0 = 0$, we remove the first two rows and columns from K'. The resulting matrix L can be shown to be non-singular.

The matrix L does not change when the lower finger contact is fixed at $\boldsymbol{p}_0$. We compute its inverse $L^{-1} = (l_{ij})$. It can be shown that $\mathcal{G}(\boldsymbol{p}_k, \boldsymbol{p}_0)$, $1 \le k \le N-1$, is a grasp if and only if $\boldsymbol{p}_0 - \boldsymbol{p}_k$ is an eigenvector of the following submatrix around the diagonal of L^{-1}:

$$\begin{pmatrix} l_{2k-1,2k-1} & l_{2k-1,2k} \\ l_{2k,2k-1} & l_{2k,2k} \end{pmatrix}.$$

Search for $\boldsymbol{p}_k$ is thus performed efficiently.

D. Large Deformation

When the object is squeezed harder, it will undergo a large deformation that needs to be modeled using the nonlinear elasticity theory. Theorem 2 is no longer applicable. The success of a grasp depends on the finger placement as well as on the finger force magnitude. To verify whether a given finger placement $\mathcal{G}(\boldsymbol{p}, \boldsymbol{q})$ is a grasp squeezing with forces of magnitude f, we need to verity conditions (1), (G1), and (G2).

For curve-like objects introduced in Section V-A, the non-linear model can be specialized from that for shells [13]. The extensional strain and the curvature variation now include some nonlinear terms:

$$\begin{aligned} \varepsilon_{11} &= \epsilon + \frac{1}{2}(\epsilon^2 + \phi^2), \\ \zeta_{11} &= (1+\epsilon)(-\beta'' - \kappa'\alpha - 2\kappa\alpha' + \kappa^2\beta) \\ &\quad -\phi(\alpha'' - \kappa'\beta - 2\kappa\beta' - \kappa^2\alpha). \end{aligned}$$

They replace ϵ and ξ respectively in the strain energy formula (4). In the FEM formulation, the strain energy becomes a quartic polynomial in terms of the nodal displacement vector Δ. The conjugate gradient method is used in the solution.

[4]The curve-like object's cross section is small enough to be viewed as a point such that a contact point is identified with the corresponding point on the object's middle curve.

VI. Simulation Results

In all simulation instances, the cross sections of the curved objects have both width and height 0.1mm, and lengths over 20mm. We let Young's modulus $E = 10^6$Pa and the coefficient of friction $\mu = 1.0$ at all contacts.

Fig. 4 shows a computed grasp $\mathcal{G}(\boldsymbol{p}, \boldsymbol{q})$ of a cubic spline, assuming small deformation of the curve. Under a squeezing

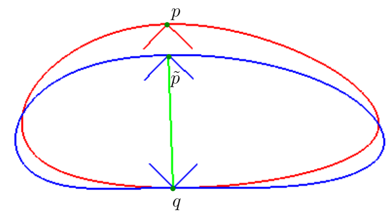

Fig. 4. Grasp $\mathcal{G}(\boldsymbol{p}, \boldsymbol{q})$ of a closed cubic spline. Friction cones are drawn at the contact points.

force of 0.3N in the direction of $\boldsymbol{q} - \boldsymbol{p}$, the upper finger contact moves from $\boldsymbol{p}$ to $\tilde{\boldsymbol{p}}$ along the line segment $\overline{\boldsymbol{pq}}$.

The first row in Table I shows pairs of boundary segments for grasp that are computed on three different shapes with perimeters 24.2mm, 35.6mm and 117.5mm, respectively. On each shape, the two segments in a pair are colored and numbered the same. Every finger location $\boldsymbol{p}$ on one segment forms a grasp with some location $\boldsymbol{q}$ on its paired segment. To better visualize the relationship, the second row in the table displays a chart for each shape which plots all such pairs $(\boldsymbol{p}, \boldsymbol{q})$ in arc length values as found by our algorithm. Given the placement of one finger, it is easy to determine that of the other using such a chart.

Due to numerical errors and computational limitation, the algorithm cannot guarantee to find all graspable segments on an object. More feasible grasps may be found with finer discretization, as shown in Fig. 5.

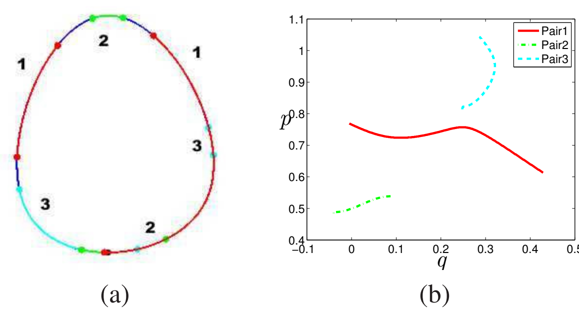

Fig. 5. Higher resolution yields one more pair of graspable segment on the second shape shown in Table I. The number of discretization points doubles from 500 to 1000.

Consider the grasp in Fig. 4. Increase the squeezing force from 0.3 to 0.6. Due to the large deformation, nonlinear elasticity theory is used in the modeling.[5] The result is shown in Fig. 6.

[5]Here, only the constraint of no rigid body rotation is imposed. The tangents of contacts are subject to change.

shape	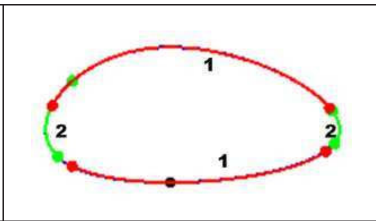			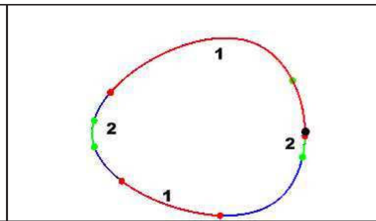			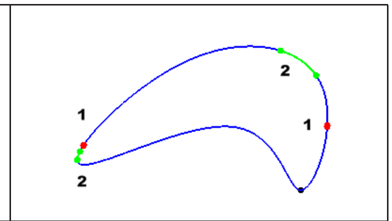		
grasp set $\{(\boldsymbol{p}, \boldsymbol{q})\}$	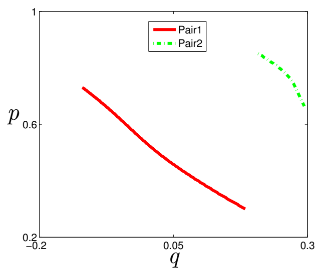			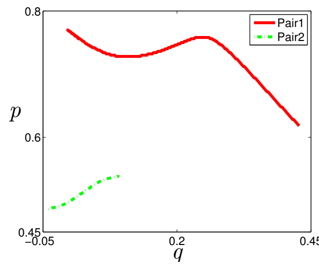			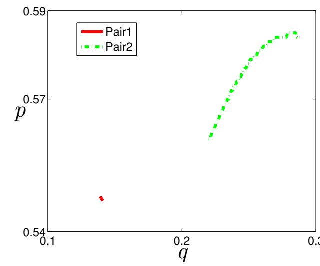		
N	500	700	1000	500	700	1000	500	700	1000
$t(s)$	137.45	467.41	1667.22	146.5	926.2	3040.9	131.5	277.3	664.4

TABLE I

GRASPABLE SEGMENTS COMPUTED ON THREE SHAPES (ROW 1) AND PLOTTED AS SETS OF FINGER LOCATIONS IN ARC LENGTH (ROW 2). THE BLACK DOT ON EACH SHAPE REPRESENTS THE POINT OF ARC LENGTH ZERO. ROWS 3 AND 4 DISPLAY VARIOUS DISCRETIZATIONS AND RESULTING EXECUTION TIMES (IN SECONDS) ON DELL OPTIPLEX 960 WITH INTEL CORE CPU OF 3.33GHZ.

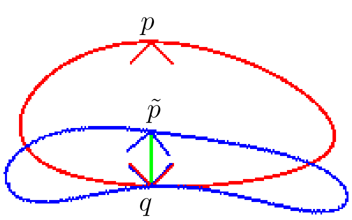

Fig. 6. The same finger placement $\mathcal{G}(\boldsymbol{q}, \boldsymbol{p})$ as in Fig. 4 retains the grasp under force of magnitude 0.6 and nonlinear elasticity modeling.

VII. DISCUSSION AND FUTURE WORK

This paper presents a preliminary study of two-finger grasps of planar deformable objects by squeezing. A grasp has to keep equilibrium before and after the deformation generated by the very set of same forces. That it seems harder to grasp a deformable object with slight force may be explained from that geometry has not changed enough to help the task.

Extension to solid planar objects is undergoing. While the presented algorithms are still applicable, the main effort is on efficiency of grasp computation.

We would like to investigate grasps yielding large deformations. Observations in our simulation suggest that one finger could often squeeze the object toward the other finger placed at one of a continuum of locations to form a grasp.

VIII. ACKNOWLEDGMENT

Support for this research was provided in part by Iowa State University, and in part by the National Science Foundation through the grant IIS-0915876.

REFERENCES

[1] A. Bicchi and V. Kumar, “Robotic grasping and contact: a review,” in *Proc. IEEE Intl. Conf. Robot. Autom.*, 2000, pp. 348–353.

[2] A. Blake, “A symmetry theory of planar grasp,” *Int. J. Robot. Res.*, vol. 14, pp. 425–444, 2004.

[3] K. Gopalakrishnan and K. Goldberg, “D-space and deform closure grasps of deformable parts,” *Int. J. Robot. Res.*, vol. 24, pp. 899–910, 2005.

[4] S. Hirai, T. Tsuboi, and T. Wada, “Robust grasping manipulation of deformable objects,” in *Proc. IEEE Symp. Assembly and Task Planning*, 2001, pp. 411-416.

[5] Y.-B. Jia, “Computation on parametric curves with an application in grasping,” *Int. J. Robot. Res*, vol. 23, pp. 825–855, 2004.

[6] Q. Luo and J. Xiao, “Geometric properties of contacts involving a deformable object,” in *Proc. IEEE Symp. Haptic Interfaces Virtual Env. Tele. Sys.*, 2006, pp. 533–538.

[7] B. Mirtich and J. Canny, “Easily computable optimum grasps in 2-D and 3-D,” in *Proc. IEEE Int. Conf. Robot. Autom.*, 1994, pp. 739–747.

[8] B. Mishra and M. Teichmann, “Three finger optimal planar grasps,” in *Proc. IEEE/RSJ Int. Conf. Intell. Robots and Systems*, 1994.

[9] V. D. Nguyen, “Constructing force-closure grasps,” *Int. J. Robot. Res.*, vol. 7, pp. 3–16, 1988.

[10] J. Ponce, S. Sullivan, J.-D. Boissonnat, and J. P. Merlet, “On characterizing and computing three- and four-finger force-closure grasps of polyhedral objects,” in *Proc. IEEE Int. Conf. Robot. Autom.*, 1993, pp. 821–827.

[11] J. Ponce, D. Stam, and B. Faverjon, “On computing two-finger force-closure grasps of curved 2D objects,” *Int. J. Robot. Res.*, vol. 12, pp. 263–273, 1993.

[12] P. R. Sinha, J. M. Abel, “A contact stress model for multifingered grasps of rough objects,” *IEEE Trans. on Robot. Automat.*, vol. 8, pp. 7–22, 1992.

[13] J. Tian and Y.-B. Jia, “Modeling deformable general parametric shells grasped by a robot hand,” *IEEE Trans. on Robot.*, vol. 26, pp. 837–852, 2010.

[14] H. Wakamatsu, S. Hirai and K. Iwata, “Static analysis of deformable object grasping based on bounded force closure,” in *Proc. IEEE/RSJ Intl. Conf. Intell. Robots and Systems*, 1996, pp. 3324-3329.

[15] H. Wakamatsu and S. Hirai, “Static modeling of linear object deformation based on differential geometry,” *Int. J. Robot. Res.*, vol. 23, pp. 293–311, 2004.